Journal of Microelectronics and Electronic Packaging (2020) **17**, 23-27

ISSN: 1551-4897

Synthesis and Characterization of Physical Properties of MgO Thin Films by Various Concentrations

Nadjat Chaouch,[1,2] Said Benramache,[2,*] and Said Lakel[3]

***Abstract*—In this work, magnesium oxide was elaborated on a glass substrate at 450°C by a pneumatic spray technique. The structural, optical, and electrical properties were studied at different MgO concentrations (.05, .10, .15, and .2 mol L^{-1}). Polycrystalline MgO films with a cubic structure with a strong (002) preferred orientation were observed at all sprayed films, with a maximum crystallite size of 21.4 nm attained by the sprayed film at .2 mol L^{-1}. Good transmission was found in the deposited MgO thin films with lowest molarity. The transmission of MgO thin films decreases rapidly as the wavelength increases in the range of 300-400 nm and then increases slowly at higher wavelengths. The bandgap of MgO thin films decreases as the molarity increases, and the band gap values range between 4.8 and 4.3 eV. The Urbach energy values range between 375 and 519 meV. The electrical resistance of our films is on the order of $2 \times 10^7 \Omega$. The prepared MgO thin films were suitable for electronic packaging; they are capable to provide very stable and high secondary electron emission combined with low bandgap energy and low electrical resistance.**

***Keywords*—MgO, thin films, MgO concentrations, pneumatic spray technique**

Introduction

In the latest research, for the important subjects in the field of materials science, the synthesis of thin films from a metal oxide (semiconductor), magnesium oxide (MgO) was used in microelectronic and optoelectronic devices because of the good dielectric constant (~9.8) and high breakdown field (12 MV cm^{-1}) when compared with the layer of silicon dioxide (SiO_2) [1, 2]. On the other hand, MgO is an important semiconductor material because of the good electrical resistance as well as excellent optical and thermodynamic stabilities [1, 2]. MgO was slightly crystallized at any temperature to the cube of the NaCl structure with lattice parameter $a = .421$ nm [1-3], The optical bandgap of MgO thin films varied between 5.6 and 7 eV [1-4] and stability was similar to that of ZnO [4]. In addition, MgO has been used in a variety of sciences and technologies, such as optoelectronic devices, because of the good structure, crystallinity, and high transparency in the visible region [5, 6]. Moreover, MgO thin films can be used in various applications, such as solar cells, chemical sensors, photodetectors, organic light-emitting diodes, IR window material, ferromagnetic thin films, ferromagnetic thin films, and protective layer in AC-plasma display panels, because of the simplicity of the synthesis [1-9].

MgO thin films can be obtained by various deposition techniques, such as reactive evaporation, electrochemical deposition, magnetron sputtering, molecular beam epitaxy, pulsed laser deposition, sol-gel process, chemical vapor deposition, and spray pyrolysis [5-12].

The aim of this work was to use a pneumatic spray technique to fabricate magnesium oxide (MgO) thin films and study the films at several MgO precursor molarities (.05, .10, .15, and .20 mol L^{-1}). The optical, electrical, and structural characterizations of magnesium oxide (MgO) thin films were investigated by using UV-visible spectrophotometry (LAMBDA 25), the four-point method, and x-ray diffraction (XRD Bruker AXS-8D), respectively.

Experiments

A. Solution Preparation

MgO solution were prepared by dissolving .05, .10, .15, and .2 mol L^{-1} of magnesium nitrate hexahydrate ($Mg(NO_3)_2.6H_2O$) in the solvent containing equal volumes of absolute H_2O adding drops of HCl to stabilize the solution. The mixture solution was stirred for 3 h at 40°C to get a clear and transparent solution.

B. Thin Film Preparation

MgO samples were fabricated by dropping MgO solution in the glass substrates at 450°C by a pneumatic spray technique, which is based on the transfer of MgO solution to the heated glass substrate in air, and we fixed the distance between the heated glass substrate and the spray solution in the gun nozzle at 17 cm, and the sample size is $0.1 \times 2.5 \times 7.5$ cm^3. The experimental conditions such as the concentration of the MgO solution, deposition rate, deposition time, substrate temperature, and final measured film thickness of MgO thin films used in this work are presented in Table I. The film thickness was measured by the weight method. MgO thin films have a nanostructure with a homogenous film thickness varied between 200 and 330 nm. MgO thin films were obtained at several MgO precursor molarities in the range of .05-.2 mol L^{-1}. A pneumatic spray

The manuscript was received on October 9, 2019; revision received on January 6, 2020; accepted on January 10, 2020
[1]Chemical Department, Faculty of Sciences, University of Batna 2, Batna 05000, Algeria
[2]Material Sciences Department, Faculty of Sciences, University of Biskra, Biskra 07000, Algeria
[3]University of Laghouat, Laghouat, Algeria
*Corresponding author; email: s.benramache@univ-biskra.dz

doi:10.4071/imaps.963453

Table I
Experimental Conditions of Deposition of MgO by Pneumatic Spray Technique

Sample Number	Concentration (mol L^{-1})	Deposition Rate (mL)	Deposition Time (min)	Deposition Temperature (°C)	Final Film Thickness (nm)
1	.05	5-10	10-13	450	~210
2	.10			450	~230
3	.15			450	~280
4	.20			450	~330

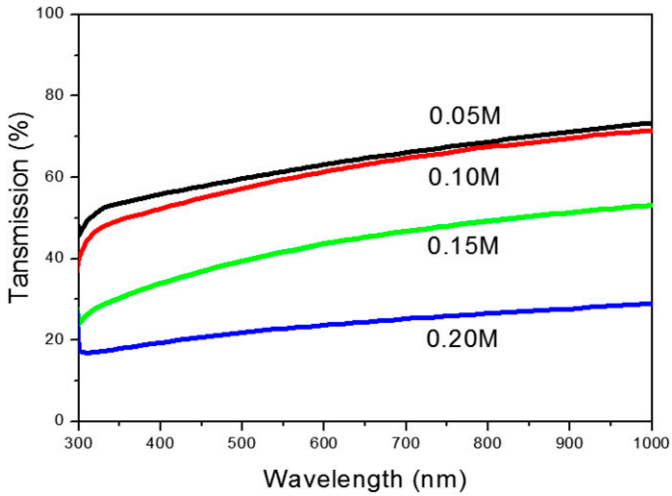

Fig. 1. Variation of transmittance spectra (T) with wavelength (λ) of MgO thin film deposited with different molarities.

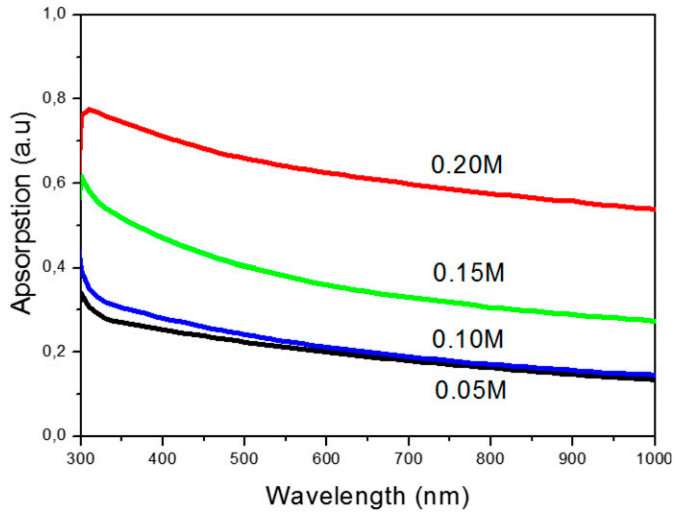

Fig. 2. Relation between absorption and wavelength of deposited MgO thin films.

Table II
Variation of Film Transmission of MgO as a Function of Molarity

Molarity (mol L^{-1})	.05	0.1	.15	0.2
Transmission (%) between 400 and 800 nm	62	59	41	22

technique was used for technological applications because it is one of the most important techniques used for deposition and large-scale production and because of low cost.

C. Thin Film Characterization

MgO thin films have been characterized to find the crystalline structure, optical transmission, and electrical conductivity by x-ray diffraction (XRD Bruker AXS-8D with $\lambda = .15406$ nm with 2θ varying between 15° and 40°), spectrophotometry (UV, Lambda 35 with 300-900 nm wavelength), and four-point method was measured by the Keithley 2400 low-voltage source meter instrument, respectively.

Results and Discussion

Fig. 1 shows the relation between transmission and wavelength in the range of 300-1,000 nm for magnesium oxide thin films. The transmission for all thin films increases as the wavelength increases in the range of 300-1,000 nm (see Table II), which corresponds to the region between the valence band and conduction band. The spectrum shows high transmission in the visible and IR regions, and low in the UV region. The transmission of MgO thin films decreases with increasing MgO precursor molarity from .05 to 0.2 M in all deposited films because of the increase in film thickness (see Table I). On the other hand, the region of the transition (absorption edge) between the valence band and the conduction band is observed between 300 and 330 nm; this attribution can be explained to find low–optical bandgap energy. Płóciennik et al. [13] have found that the absorption edge of MgO films is about 160 nm. We observed the effect of MgO precursor molarity on the optical property.

Reflectance R can be obtained from the absorption and transmission spectrum in accordance with the law of conservation of energy by the relation [14]:

$$R + T + A = 1, \tag{1}$$

where R is the reflectance, T is the transmission of the films, and A is the absorption. In Fig. 2, it be noticed that all the prepared thin films have different absorption in the visible range of the spectrum, which shows the relation between absorption (A) and transmission (T). The high absorption edge value can be found with 0.2 M because of the increase in the film thickness.

The optical energy gap (E_g) was derived assuming direct transitions between the edge of the valence and conduction bands. For MgO thin films, we can calculate using Tauc's equation [15]

$$(\alpha h\nu) = C(h\nu - Eg)^n, \tag{2}$$

Table III
Variation of the Optical Bandgap Energy E_g and the Urbach Energy of MgO Thin Films with Different Molarities

Molarity (mol L^{-1})	Optical gap energy E_g(eV)	Urbach energy E_u (meV)	Refractive index (n)
.05	4.77	519	1.8
.10	4.48	465	1.9
.15	4.42	420	2.2
.20	4.28	375	2.4

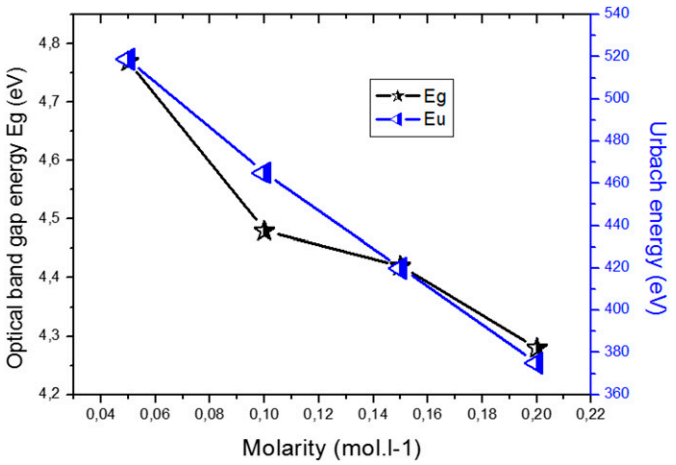

Fig. 3. Variation of optical bandgap and Urbach energy of MgO thin films as a function molarity.

Table IV
Electrical Resistance of MgO Thin Films with Different Molarities

Molarity (mol L^{-1})	.05	.10	.15	.20
I (A) $\times 10^{-6}$	0.5	0.5	0.5	0.5
V_1 (V)	.0712	.0542	.0473	.0325
V_1 (V)	.0290	.0473	.0277	.398
V_3 (V)	.0640	.0521	.0455	.217
R_{sh} (Ω) $\times 10^7$	2.18	2.11	1.87	1.68

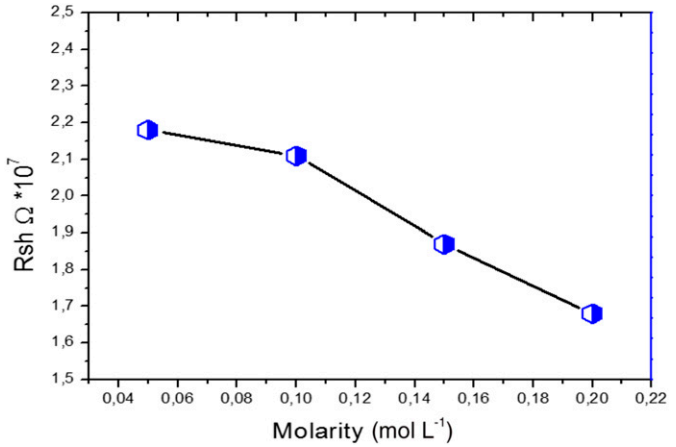

Fig. 4. Electrical resistivity variations with different molarities of MgO thin films.

where α is the absorption coefficient, C is a constant, $h\nu$ is the energy of incident photon, and n depends on the quantum selection rules for different materials, which may equal to 1/2 for direct and 2 for indirect bandgap. In our case, we have used n = 1/2 because it gives an excellent linear fitting curve in the band-edge region [16].

The absorbance ($\alpha d = 2.303A$) has been used to determine the bandgap of the evolving MgO film by measuring the absorption coefficient as a function of the incident photon energy ($h\nu$).

The graphs of $(\alpha h\nu)^2$ versus ($h\nu$) plots of MgO films fabricated at different molarities were obtained. Bandgap energy E_g can be obtained by extrapolation of the linear portion of the graph to the energy axis at $\alpha = 0$ [15] in the range between 300 and 330 nm as shown in Table III.

In addition, we have used the tail width, which can be calculated using the Urbach rule for the absorption coefficient at lower photon energy [17].

$$\alpha(h\nu) = \alpha_0 \exp\left(\frac{h\nu}{E_u}\right), \tag{3}$$

where α_0 is the constant and E_u is the Urbach energy. Variation of the graph of Ln α versus (hν) plots is used to deduce the Urbach energy of MgO thin films; these values are given in Table III.

Table III gives the values of E_g and E_u at different concentrations of molarities of MgO solution. On the other hand, Fig. 3 shows the variation of optical bandgap and Urbach energy of MgO thin films as a function of molarity. As can be seen, bandgap energy E_g and Urbach energy E_u are dependent on the change in MgO solution. It is clear that the values of E_g are in agreement with E_u variation. However, it can be observed that the bandgap energy of MgO thin films decreased slowly with increasing MgO molarity. This result can be explained by the increase in oxygen with the film preparation as mentioned earlier. As a result, both decrease in the optical gap and broadening of the Urbach tail occurred. Similar to our findings, El-Gamal and El Sayed [18] obtained that the optical gap energy of PAM/PVA-loaded MgO NPs varied between 4.4 and 5.3 eV. However, Ibrahim [19] have the highest value of Urbach energy that was found in the range of 1.8-4.2 eV.

Refractive index (n) of MgO thin films was calculated by using the following equation [20]:

$$n = \frac{(1+R)}{(1-R)} + \sqrt{\frac{4R}{(1-R)^2} - K^2}, \tag{4}$$

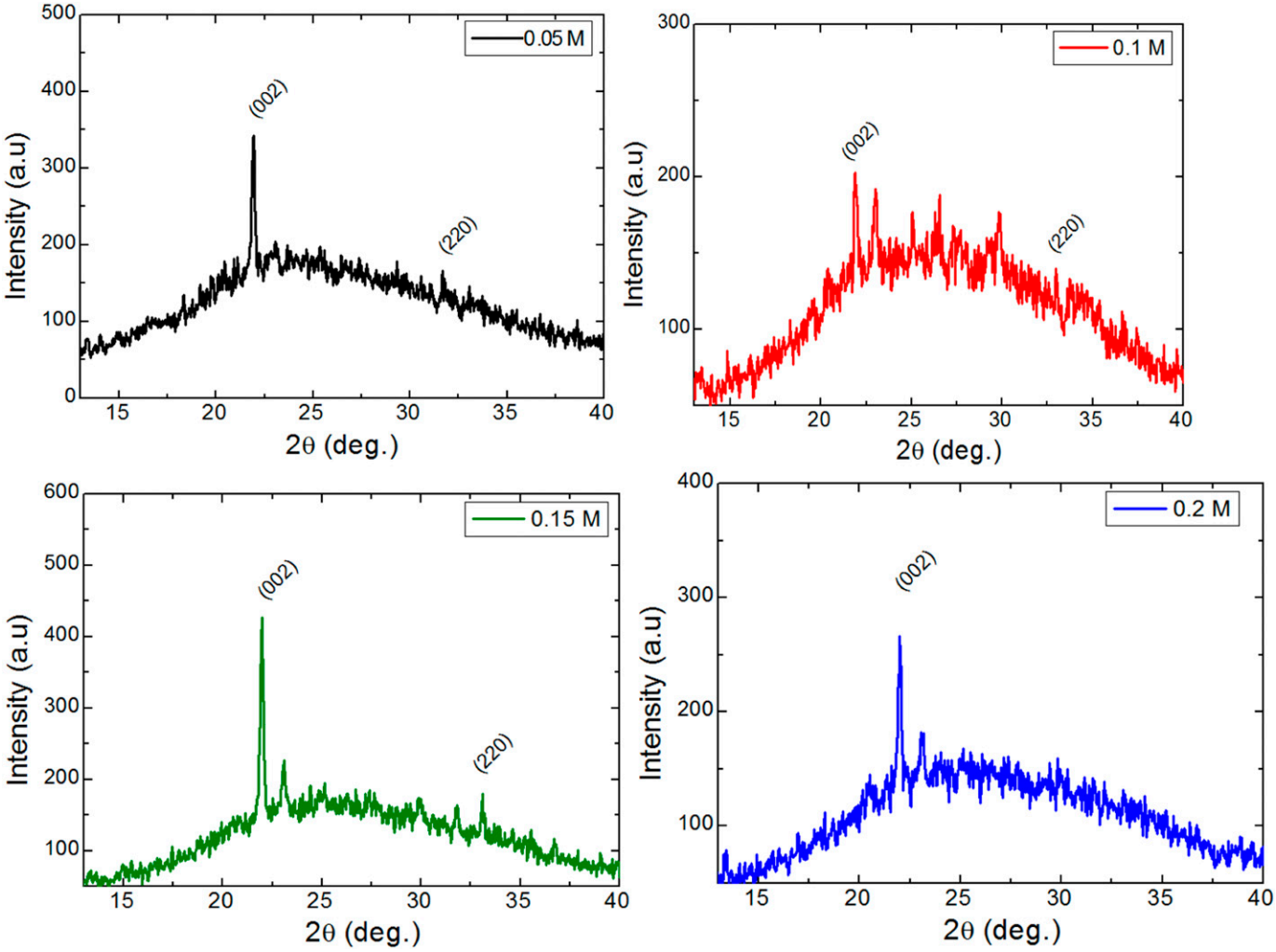

Fig. 5. XRD spectra of MgO thin films deposited with different molarities.

where R is the reflectance and K is the extinction coefficient of MgO thin films. The extinction coefficient was determined from by the following relation [20]:

$$k = \frac{\alpha\lambda}{4\pi}, \tag{5}$$

where λ is the wavelength and α is the absorption coefficient. The refractive index n is presented in Table III. We have observed that the value is smaller than 2.4. Mousa et al. [21] found that the deposited MgO thin films at 450°C have a refractive index of about 3.1.

The four-point probe is required to measure the sheet resistance of the films. Because negligible contact and spreading resistance are associated with voltage probes, the sheet resistance (R_{Sh}) can be estimated, when the film thickness is less than the distance between the probes, using the following relation [22]:

$$R_{sh} = \frac{\pi}{\ln(2)} \times \frac{V}{I}, \tag{6}$$

where I is the applied current and V is the measurement voltage.

Table IV and Fig. 4 give R_{sh} values of MgO thin films as a function of concentration molarity. As can be seen that R_{sh} was found to be decreasing with the increasing concentration molarity. The decrease in the resistance can be explained by the increase in the film thickness of the deposited MgO thin films with different molarity.

The effect of MgO concentration on the crystal structure and preferred orientations of the sprayed MgO thin films were characterized by the XRD technique. Fig. 5 shows the XRD patterns of MgO thin films deposited with various concentrations of .05, .10, .15, and .2 mol L^{-1}. As the first result, all the films exhibited two diffraction peaks at $2\theta = 22$ and 31° relative to (002) and (220) planes of the MgO phase, indicating that MgO thin films have a polycrystalline cubic structure. The good crystal structure showed a strong peak, which corresponded to the (002) plane of the MgO cubic structure. It can be seen that the intensity of the (002) peak of the sprayed MgO thin film with .15 M has a good crystallinity, which confirmed the improvement of the crystalline quality and the reduction of defects in the crystal structure. The lattice parameter a of MgO thin films was found on order to .421 nm, which is in agreement with that obtained in [18-21].

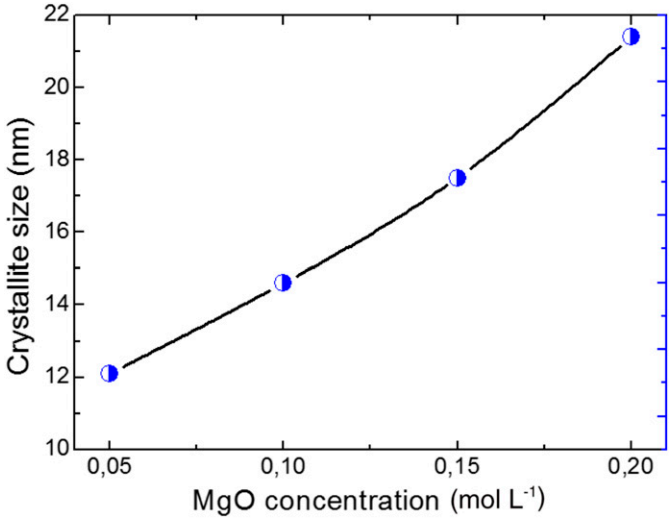

Fig. 6. Variation of the crystallite size of MgO thin films deposited with different molarities.

The crystallite size G of (002) diffraction peak of MgO thin films was calculated using Scherrer's equation [23]:

$$G = \frac{.9\lambda}{\beta \cos\theta}, \quad (7)$$

where G is the crystallite size, λ is the wavelength of x-ray (λ = 1.5418 A°), β is the full width at half maximum, and θ is the angle of the diffraction peak. Fig. 6 shows the variations of the crystallite size of the (002) diffraction peak as a function of MgO concentration. It can be seen that the crystallite size increased with the increasing MgO concentration from 12.1 nm for .05 to 21.4 nm for .20 mol L^{-1}, which may be due to the improvement of the crystalline quality of MgO.

Conclusion

In this study magnesium oxide thin films were deposited on a glass substrate by a pneumatic spray technique. The effects of the concentration molarity (.05, .1, .15, and 0.2 M) were successfully investigated. High transmission was found in the deposited MgO thin film with lowest molarity. The transmittance of MgO thin films decreases rapidly as the wavelength increases in the range of 300-400 nm and then increases slowly at higher wavelengths. The bandgap of MgO thin films decreases as the molarity increases, and the bandgap values range between 4.8 and 4.3 eV. The Urbach energy values range between 375 and 519 meV. The electrical resistance of our films is on the order $2 \times 10^7 \Omega$. Polycrystalline MgO films with a cubic structure with a strong (002) preferred orientation were observed at all sprayed films, with a maximum crystallite size of 21.4 nm attained by the sprayed film at .2 mol L^{-1}. A good transmission was found in the deposited MgO thin film with lowest molarity.

References

[1] P. Maiti, P.S. Das, M. Bhattacharya, S. Mukherjee, B. Saha, A.K. Mullick, and A.K. Mukhopadhyay, "Transparent Al^{+3} doped MgO thin films for functional applications," *Materials Research Express*, Vol. 4, p. 086405, 2017.

[2] Z. Bazhan, F.E. Ghodsi, and J. Mazloom, "Effect of stabilizer on optical and structural properties of MgO thin filmsprepared by sol–gel method," *Bulletin of Materials Science*, Vol. 36, pp. 899-905, 2013.

[3] D.K. Fork, F.A. Ponce, J.C. Tiramontana, and T.H. Geballe, "Epitaxial MgO on Si(OO1) for Y-Ba4U0 thin-fil growth by pulsed laser deposition," *Applied Physics Letters*, Vol. 58, pp. 2294-2296, 1991.

[4] S.G. Khalil, M.M. Mutter, Z.K. Mohammed, and G. Salem, "Fabrication and characterization of gas sensor from ZrO2: MgO nanostructure thin films by R.F. magnetron sputtering technique," *Baghdad Science Journal*, Vol. 16, pp. 199-208, 2019.

[5] S. Iacobucci, F. Offi, P. Torelli, and L. Petaccia, "Effective attenuation lengths of low energy electrons in MgO thin films," *Journal of Electron Spectroscopy and Related Phenomena*, Vol. 233, pp. 1-4, 2019.

[6] G. Suárez-Campos, D. Cabrera-German, J.A. García-Valenzuela, M. Cota-Leal, J.L. Fuentes-Ríos, M. Martínez-Gil, H. Hu, and M. Sotelo-Lerma, "Controlled synthesis of Mg(OH)2 thin films by chemical solution deposition and their thermal transformation to MgO thin films," *Ceramics International*, Vol. 45, pp. 10356-10363, 2019.

[7] Z. Mohammed, S. Khalil, and M. Mutter, "Synthesis and characterization of ZrO2: MgO thinfilms by plasma of R.F. magnetron sputtering," *Karbala International Journal of Modern Science*, Vol. 5, No. 1, p. A3, 2019.

[8] İ.A. Kariper and F.M. Tezel, "UV region supercapacitor: Bi-doped natural MgO rock salt thin film," *Ceramics International*, Vol. 45, pp. 9219-9224, 2019.

[9] S. Tigunta, P. Khlikhum, P. Kidkhunthod, N. Chanlek, L. Supadee, and S. Pojprapai, "Dissolution behavior of MgO thin film-barrier magnetic tunneling junctions," *Journal of Materials Science Materials in Electronics*, Vol. 30, pp. 6718-6724, 2019.

[10] T. Komori, A. Anzai, T. Gushi, K. Toko, and T. Suemasu, "Molecular beam epitaxy growth of Mn4−xNixN thin films on MgO(0 0 1) substrates and their magnetic properties," *Journal of Crystal Growth*, Vol. 507, pp. 163-167, 2019.

[11] I. Cora, Z. Baji, Z. Fogarassy, Z. Szabó, and B. Pécz, "Structural study of MgO and Mg-doped ZnO thin films grown by atomic layer deposition," *Materials Science in Semiconductor Processing*, Vol. 93, pp. 6-11, 2019.

[12] H. Güney and D. İskenderoğlu, "Synthesis of MgO thin films grown by SILAR technique," *Ceramics International*, Vol. 44, pp. 7788-7793, 2018.

[13] P. Płóciennik, D. Guichaoua, A. Zawadzka, A. Korcala, J. Strzelecki, P. Trzaska, and B. Sahraoui, "Optical properties of MgO thin films grown by laser ablation technique," *Optical and Quantum Electronics*, Vol. 48, p. 277, 2016.

[14] Y.P. Santos, E. Valença, R. Machado, and M.A. Macêdo, "A novel structure ZnO-Fe-ZnO thin film memristor," *Materials Science in Semiconductor Processing*, Vol. 86, pp. 43-48, 2018.

[15] S. Benramache, B. Benhaoua, N. Khechai, and F. Chabane, "Elaboration and characterisation of ZnO thin films," *Matériaux & Techniques*, Vol. 100, pp. 573-580, 2012.

[16] Y. Aoun, M. Marrakchi, S. Benramache, B. Benhaoua, S. Lakel, and A. Cheraf, "Preparation and characterizations of monocrystalline Na doped NiO thin films," *Materials Research*, Vol. 21, p. e20170681, 2018.

[17] A. Diha, S. Benramache, and L. Fellah, "The crystalline structure, optical and conductivity properties of fluorine doped ZnO nanoparticles," *Journal of Nano and Electronics Physics*, Vol. 11, p. 03002, 2019.

[18] S. El-Gamal and A.M. El Sayed, "Physical properties of the organicpolymeric blend (PVA/PAM)modified with MgO nanofillers," *Journal of Composite Materials*, Vol. 53, pp. 831-2847, 2019.

[19] F.T. Ibrahim, "Characterization of pulsed-laser deposited CuO-doped MgO thin filmsfor gas sensing applications," *Iraqi Journal of Applied Physics*, Vol. 13, pp. 13-17, 2017.

[20] S. Gupta, A. Paliwal, V. Gupta, and M. Tomar, "Surface plasmon resonance assisted optical analysis of strontium barium niobate thinfilms," *Applied Surface Science*, Vol. 501, p. 144178, 2020.

[21] A.O. Mousa, N.A. Nema, and S.H. Trier, "Study of structural and optical properties for MgO films prepared by using chemical spray pyrolysis technique," *Materials Science: An Indian Journal*, Vol. 14, pp. 426-434, 2016.

[22] A. Rahal, A. Benhaoua, C. Bouzidi, B. Benhaoua, and B. Gasmi, "Effect of antimony doping on the structural, optical and electrical properties of SnO2 thin films prepared by spray ultrasonic," *Superlattices and Microstructures*, Vol. 76, pp. 105-114, 2014.

[23] K. Kandpal and N. Gupta, "Study of structural and electrical properties of ZnO thin film for thin film transistor (TFT) applications," *Journal of Materials Science Materials in Electronics*, Vol. 28, pp. 16013-16020, 2017.